BIOLOGY OF REPRODUCTION (2014) **91**(2):34, 1–12
Published online before print 11 June 2014.
DOI 10.1095/biolreprod.113.115717

Ovarian Membrane-Type Matrix Metalloproteinases: Induction of MMP14 and MMP16 During the Periovulatory Period in the Rat, Macaque, and Human[1]

Muraly Puttabyatappa,[3] Terry A. Jacot,[4] Linah F. Al-Alem,[3] Katherine L. Rosewell,[3] Diane M. Duffy,[5] Mats Brännström,[6] and Thomas E. Curry, Jr.[2,3]

[3]*Department of Obstetrics and Gynecology, Chandler Medical Center, University of Kentucky, Lexington, Kentucky*
[4]*Department of Obstetrics and Gynecology, Eastern Virginia Medical School, Norfolk, Virginia*
[5]*Department of Physiological Sciences, Eastern Virginia Medical School, Norfolk, Virginia*
[6]*Department of Obstetrics and Gynecology, Sahlgrenska Academy, University of Gothenburg, Gothenburg, Sweden*

ABSTRACT

An intrafollicular increase in proteolytic activity drives ovulatory events. Surprisingly, the periovulatory expression profile of the membrane-type matrix metalloproteinases (MT-MMPs), unique proteases anchored to the cell surface, has not been extensively examined. Expression profiles of the MT-MMPs were investigated in ovarian tissue from well-characterized rat and macaque periovulatory models and naturally cycling women across the periovulatory period. Among the six known MT-MMPs, mRNA expression of *Mmp14*, *Mmp16,* and *Mmp25* was increased after human chorionic gonadotropin (hCG) administration in rats. In human granulosa cells, mRNA expression of *MMP14* and *MMP16* increased following hCG treatment. In contrast, mRNA levels of *MMP16* and *MMP25* in human theca cells were unchanged before ovulation but declined by the postovulatory stage. In macaque granulosa cells, hCG increased mRNA for *MMP16* but not *MMP14*. Immunoblotting showed that protein levels of MMP14 and MMP16 in rats increased, similar to their mRNA expression. In macaque granulosa cells, only the active form of the MMP14 protein increased after hCG, unlike its mRNA or the proprotein. By immunohistochemistry, both MMP14 and MMP16 localized to the different ovarian cell types in rats and humans. Treatment with hCG resulted in intense immunoreactivity of MMP14 and MMP16 proteins in the granulosa and theca cells. The present study shows that MMP14 and MMP16 are increased by hCG administration in the ovulating follicle, demonstrating that these MMPs are conserved among rats, macaques, and humans. These findings suggest that MT-MMPs could have an important role in promoting ovulation and remodeling of the ovulated follicle into the corpus luteum.

extracellular matrix, granulosa cells, matrix metalloproteinase, ovary, ovulation, theca cell

INTRODUCTION

Expulsion of the oocyte during the process of ovulation is a crucial event in the reproductive cycle of all mammalian species. A key facilitator of this process is increased proteolytic activity in the periovulatory follicle, which is brought about by the luteinizing hormone (LH) surge or exogenous human chorionic gonadotropin (hCG) administration [1]. Some of the proteases induced during the periovulatory period are members of the MMP (matrix metalloproteinase), plasminogen activator/plasmin, and ADAMTS (a disintegrin and metalloprotease with thrombospondin-like motifs) families [2–5]. These proteases are hypothesized to bring about the breakdown of the follicular wall and surrounding matrix to allow expulsion of the oocyte. The importance of these enzymes is highlighted by studies that show administration of specific protease inhibitors or deletion of the ADAMTS1 gene can block ovulation [5–7].

Proteinases of the MMP family belong to the superfamily of structurally related zinc endopeptidases that are collectively referred to as metzincins [8]. These family members are usually secreted as proproteins into the extracellular matrix, where they are activated as a result of cleavage by other proteases, including MMPs. Activated MMPs can not only degrade a variety of extracellular matrix components but also act on other proteins, such as growth factors, growth factor binding proteins, and protease inhibitors [9]. Therefore, MMPs can influence a wide array of cellular functions, including cell invasion, cell migration, apoptosis, and angiogenesis [10]. Approximately 25 forms of vertebrate MMPs and 22 human homologs are known. These are classified into four broad subfamilies based on their gene structure [11]. Group 1 consists of the collagenase subfamily. Group 2 consists of the gelatinase subfamily that contains fibronectin-like domains. Group 3 consists of MMPs with a variant hemopexin exon. Group 4 consists of MMPs with a variant catalytic exon and a unique 3′-end exon containing plasma membrane and cytoplasmic domains; this last subfamily consists of the MMPs that are called the membrane-type (MT) MMPs.

The MT-MMPs are unique in that unlike other MMPs, they are not secreted into the extracellular space but instead are inserted into or anchored onto the cell membrane. This family has six members, named sequentially as MT1-MMP (MMP14), MT2-MMP (MMP15), MT3-MMP (MMP16), MT4-MMP (MMP17), MT5-MMP (MMP24), and MT6-MMP (MMP25) [11, 12]. Among these MMPs, the type I MT-MMPs (MMPs 14–16 and 24) have a transmembrane domain and an intracytoplasmic domain, whereas the type II MT-MMPs (MMPs 17 and 25) have a glycosylphosphatidylinositol (GPI) link domain through which they are anchored onto the cell membrane. All MT-MMPs, by virtue of their presence on the membrane, are thought to participate in pericellular proteolysis of matrix proteins to promote cell growth/expansion and migration or cancer metastasis [12]. In addition, these proteases can cleave proforms of other enzymes, including secreted pro-

[1]Supported by National Institutes of Health Grants P20 RR15592 (T.E.C.), HD057446 (T.E.C.), and HD054691 (D.M.D.), and the Swedish Research Council (11607, M.B.).
[2]Correspondence: Thomas E. Curry, Jr., Department of Obstetrics and Gynecology, Chandler Medical Center, 800 Rose Street, Room MS 331, University of Kentucky, Lexington, Kentucky 40536-0298.
E-mail: tecurry@uky.edu

Received: 7 November 2013.
First decision: 4 December 2013.
Accepted: 2 June 2014.

eISSN: 1529-7268 http://www.biolreprod.org
ISSN: 0006-3363

MMPs contributing to their activation or growth factors to influence cell function.

Biomedical research involves the use of animal models, such as rodents or nonhuman primates, to perform experiments that otherwise cannot be done on humans because of ethical considerations. The data derived from these animal models must mimic changes observed in humans. This allows extrapolation and interpretation of the laboratory animal data during either physiological or pathological conditions in humans. The present comparative study was therefore undertaken to determine the expression profile of MT-MMPs utilizing well-characterized experimental rat and macaque models of ovulation. The data from these species were then compared with observations in ovarian tissues collected across the periovulatory period from women. In addition, whereas the expression profiles of other groups of MMPs in the ovary of various species during the periovulatory period have been reported [3], the expression profiles of the MT-MMPs have not been thoroughly explored in mammalian follicles. Therefore, we report, to our knowledge for the first time, that specific MT-MMPs are induced in the ovarian cells of rats, cynomolgus macaques, and humans by an ovulatory stimulus.

MATERIALS AND METHODS

Rat Ovarian Tissue Collection

Immature female Sprague-Dawley rats (Harlan Sprague-Dawley, Inc.) were maintained at room temperature with food and water provided ad libitum. Rats were administered 10 IU of equine chorionic gonadotropin (eCG) s.c. at 22–23 days of age to stimulate ovarian follicular development. Forty-eight hours after eCG injection, ovulation was induced by administering 5 IU of hCG. For tissue collection, rats were euthanized at defined intervals after hCG treatment (0, 4, 8, 12, and 24 h). Whole ovaries were frozen for mRNA and protein analysis or fixed in neutral buffered formalin for localization studies. Ovaries were also used to collect granulosa cells and residual ovarian tissue as outlined below. The residual ovarian tissue represents the tissue remaining after granulosa cell collection and is comprised of theca, interstitial, endothelial, and stromal cells as well as remaining granulosa cells. For collection of granulosa cells and residual tissue, ovaries were punctured with a 26-gauge needle to release granulosa cells and cumulus-oocyte complexes (COCs) into a Petri dish containing Opti-MEM media (Life Technologies). The remaining residual ovarian tissue was removed, and granulosa cells were partially purified by filtration through a nylon filter (pore size, 40 μm) to remove large tissue debris and COCs. The cells were then pelleted by centrifugation at $300 \times g$ and stored at −70°C until further analysis. All animal procedures for these experiments were approved by the University of Kentucky Institutional Animal Care and Use Committee.

Macaque Ovarian Tissue Collection

Granulosa cells and whole ovaries were obtained from adult female cynomolgus macaques at Eastern Virginia Medical School. A controlled ovarian stimulation model developed to collect multiple oocytes for in vitro fertilization was used to obtain monkey granulosa cells [13]. Beginning within 3 days of initiation of menstruation, recombinant human (r-h) follicle-stimulating hormone (FSH; 90 IU daily; Organon) was administered for 6–8 days followed by daily administration of 90 IU of r-hFSH plus 60 IU of r-hLH (Serono Reproductive Biology Institute) for an additional 2 days to stimulate the growth of multiple preovulatory follicles. A gonadotropin-releasing hormone (GnRH) antagonist (either Ganirelix [30 μg/kg body wt; Schering-Plough] or Antide [0.5 mg/kg body wt; Serono]) was also administered daily to prevent an endogenous ovulatory LH surge. At the end of this treatment regimen, ovulation was induced by administration of 1000 IU of r-hCG (Serono) [14]. Follicular aspiration was performed during aseptic laparotomy before (0 h) or 12, 24, or 36 h after hCG administration. To obtain granulosa cells, each follicle was pierced with a 22-gauge needle, and the aspirated contents of all follicles larger than 4 mm in diameter were pooled. Monkey granulosa cells and oocytes were pelleted from the follicular aspirates by centrifugation at $300 \times g$. Following oocyte removal, a granulosa cell-enriched population of the remaining cells was obtained by Percoll gradient centrifugation [2]. Granulosa cells obtained were frozen in liquid nitrogen and stored at −80°C for preparation of total RNA. For protein analysis, cells were lysed in 1% Triton X-100/0.5% SDS and total protein quantitated. Whole ovaries were also obtained from monkeys undergoing ovarian stimulation as described above. Ovaries were bisected, maintaining at least two periovulatory follicles greater than 4 mm in diameter on each piece. The pieces were embedded in O.C.T. Compound (Sakura), frozen in liquid propane, and stored at −80°C. All animal protocols and experiments were approved by the Eastern Virginia Medical School Animal Care and Use Committee and were conducted in accordance with the National Institutes of Health (NIH) Guide for the Care and Use of Laboratory Animals.

Human Granulosa and Theca Cell Collection

Human ovarian granulosa and theca cells were collected before and at different times after ovulatory hCG treatment as described previously [15]. Briefly, women undergoing tubal sterilization were recruited and monitored by transvaginal ultrasound for two or three menstrual cycles to insure normal follicular growth and ovulation. Women with normal menstrual cycles were monitored with repeated transvaginal ultrasound to enable surgery at a stage when the dominant follicle was preovulatory. For samples collected at the preovulatory phase, surgery was performed before the LH surge when the dominant follicle was between 14 and 17.5 mm. The remaining patients received an injection of r-hCG (250 μg; Ovitrelle; EMD Serono) to mimic the endogenous LH surge. Subsequently, patients underwent surgery at varying times after hCG injection: early ovulatory phase (from 12 to 18 h), late ovulatory phase (from >18 to 34 h), and postovulatory phase (from >44 to 70 h). The intact dominant follicle was excised and either fixed in neutral buffered formalin and embedded in paraffin for immunolocalization or granulosa and theca cells were isolated and frozen for subsequent mRNA expression analysis by real-time RT-PCR. Theca cells were obtained from all four periovulatory phases, but granulosa cells could not be collected from the postovulatory group due to a loss of cells after ovulation. This study was approved by the human ethics committee at the University of Gothenburg, and informed written consent was obtained from all patients before surgery.

Real-Time RT-PCR

Total RNA was isolated using TRIzol reagent (Invitrogen) from intact rat ovaries or the residual tissue. An RNeasy mini kit (Qiagen) was used to isolate RNA per the manufacturer's guidelines. Total RNA (1 μg) was reverse transcribed into cDNA for use in the gene expression analysis.

The mRNA expression of the different MT-MMPs in the rat and human samples was analyzed using TaqMan Gene Expression Assays (Life Technologies). The following assay-on-demand primer-probe sets from Applied Biosystems were used: for human gene expression analysis, Hs00237119_m1 (*MMP14*), Hs00234670_m1 (*MMP16*), Hs01554789_m1 (*MMP25*), and 4326317E (*GAPDH*); for rat gene expression analysis, Rn00579172_m1 (*Mmp14*), Rn01536925_m1 (*Mmp15*), Rn00679255_m1 (*Mmp16*), Rn01499864_m1 (*Mmp17*), Rn00582144_m1 (*Mmp24*), Rn01471830_m1 (*Mmp25*), and Rn00820748_g1 (*Rpl32*). The target gene and the control gene real-time analyses were carried out in the same reaction.

Oligonucleotide primers corresponding to cDNA for *Macaca* MMP14 (GenBank Accession #XM_001266810; forward, 5′-CTTGCTTAGTCAGT CAAGTTCC-3′; reverse, 5′-CATCCAAGGCTAACATTCG-3′) and *Macaca* MMP16 (GenBank Accession #XM_001084206; forward, 5′-GACAGGACA GAAGTGGCAGC-3′; reverse, 5′-AAAGGCACGGCGAATAGC-3′) were designed using PRIMER3 software (part of Biology Work Bench Version 3.2; http://workbench.sdsc.edu/), and the specificity for each primer set was confirmed by both electrophoresis of the PCR products and analysis of the melting (dissociation) curve after each real-time PCR reaction. The changes in *MMP25* mRNA expression were not assessed in the cynomolgus macaque samples because we could not validate the primers in ovarian samples using primers designed using the rhesus macaque sequence in the National Center for Biotechnology Information database or utilizing commercially available primers for rhesus macaque (from Applied Biosystems). PCR reactions were performed on a Mx3000P 124 QPCR System (Stratagene). The relative amount of each MMP transcript was calculated using the $\Delta\Delta C_T$ method and normalized to the endogenous reference gene GAPDH (in human samples) and RPL32 (in macaque and rat samples) as previously described [16].

Immunoblotting

Monkey granulosa or rat whole-ovarian lysates (20 μg of total protein) were denatured and reduced by heating in Laemmli buffer containing 50 mM dithiothreitol for 5 min at 95°C. The lysates were then run on 10% SDS-PAGE gels and transferred onto a polyvinylidene fluoride membrane. Membranes were blocked with 5% skim milk in Tris-buffered saline containing 0.05%

Tween 20 (TBST). Incubation with either MMP14 or MMP16 primary antibodies (Triple Point Biologics) was done at 4°C overnight. Washed blots were incubated with respective secondary antibody conjugated with horseradish peroxidase against the host species at room temperature. Blots were washed five times with TBST and bands visualized using an Amersham ECL Advance Kit (GE Healthcare) on a chemiluminescent film (Sigma-Aldrich). Using the ImageJ software (Version 1.46; NIH), the immunoblots were quantitated by determining relative optical density units.

Immunofluorescence

Frozen monkey ovarian tissues were sectioned (thickness, 10 μm) and fixed with buffered 10% formalin. After antigen retrieval with 10 mM sodium citrate (pH 6), sections were treated with Image-it FX (Invitrogen) according to manufacturer's instructions, then blocked with 5% nonimmune horse serum (Vector Laboratories) in phosphate-buffered saline containing 0.1% Triton. Sections were incubated for 2 h at room temperature either with primary antibody (Abcam) generated against MMP14 or MMP16 or with no primary antibody followed by 1-h incubation with species-appropriate Alexa Fluor 488-conjugated secondary antibody (Molecular Probes). The slides were coverslipped using VECTASHIELD medium containing propidium iodide (Vector Laboratories). For immunodetection of MMPs 14, 16, and 25, from 8 to 12 sections were used for each time point. All images were obtained using an Olympus BX41 fluorescent microscope fitted with a DP70 digital camera and associated software (Olympus).

Immunohistochemistry

Immunohistochemistry for the MT-MMPs in humans and rats was performed using Starr Trek Universal HRP Detection System (Biocare) as previously reported [17]. Briefly, paraffin-embedded sections (thickness, 7 μm) of human follicles or rat ovaries were deparaffinized for 10 min in xylene followed by a decreasing ethanol series and three washes in Tris-buffered saline (TBS). The endogenous peroxide activity was then quenched with Peroxidazed 1 (Biocare) treatment for 5 min. Antigen retrieval was accomplished using DakoCytomation Target Retrieval Solution (Dako North America, Inc.) for 20 min at 100°C, after which the slides were allowed to come to room temperature, washed once in TBS, and then blocked for 10 min with Background Sniper (Biocare). Sections were incubated with MMP14, MMP16, or MMP25 antibodies (Triple Point Biologics) at 4°C overnight, washed in TBS, and incubated with biotinylated secondary antibody for 2 h. To amplify the reaction signal, the sections were treated with a conjugated streptavidin alkaline phosphatase (TrekAvidin-AP Label; Biocare) for 10 min before staining, then visualized using a Vulcan Fast Red Chromagen (Biocare), counterstained with hematoxylin, and coverslipped using VectaMount mounting media (Vector Laboratories). In control sections, primary antibody was omitted. For immunodetection of MMPs 14, 16, and 25, a total of 25 sections each were used for 0 and 12 h in rats and 27 sections for the preovulatory stage and 10 sections for the late ovulatory stage in humans. All images were obtained using a Nikon Eclipse E800 microscope fitted with a DSRi1 digital camera and associated software NIS Elements AR version 3.10 (Nikon).

Statistical Analysis

All data were checked for heterogeneity of variance using Bartlett chi-square test. Data with heterogenous variances were log transformed for analysis. To avoid bias by choosing one sample as a control to calculate the fold-change where appropriate, a mean of the $\Delta\Delta C_T$ of all the control samples was used to set the value at one. This led to different values for our controls that were still close to one; as a result, the controls have error bars. Changes in gene expression and densitometric values from MT-MMP immunoblots were analyzed by one-way ANOVA followed by Bonferroni post-hoc tests. All analyses were performed using GraphPad Prism (Version 5.00; GraphPad Software, Inc.). Differences were considered to be significant at $P < 0.05$. Graphs were plotted using the mean ± SEM for each data point with GraphPad Prism software.

RESULTS

Messenger RNA Expression Profile of MT-MMPs During the Periovulatory Period

The mRNA expression profiles for five of the MT-MMPs in intact rat ovaries, granulosa cells, and residual tissues are depicted in Figure 1. The mRNA expression profile of *Mmp14* increased by 8 h post-hCG in rat granulosa cells, but no change was observed in the intact rat ovary and residual ovarian tissue (Fig. 1A). This increase was observed before ovulation, which occurs 14–16 h after hCG administration in this model [18]. The expression of *Mmp16* increased by 15-fold at 12 h after hCG administration in rat granulosa cells but showed no change in the intact ovary (Fig. 1B). In contrast to the granulosa cells, *Mmp16* mRNA in the rat residual ovarian tissue declined by 8 h post-hCG and stayed low until 24 h. The mRNA levels for *Mmp25* in the intact rat ovary and granulosa cells peaked by 8 h after hCG and declined thereafter, but no change was observed in the residual ovarian tissue (Fig. 1C). The mRNA for *Mmp15* and *Mmp17* was detectable in the intact rat ovary, granulosa cells, and residual ovarian tissue, but no change was evident after hCG administration (Fig. 1, D and E). Among the MT-MMPs, mRNA for *Mmp24* was below the detectable limit in the rat ovary at all time points before or after hCG (data not shown)

We focused our attention on gene expression profiles for MMPs 14, 16, and 25 in the human and macaque species because these mRNAs increased significantly during the rat periovulatory period and also because of the limited availability of samples from these species. Human granulosa and theca cells collected from different stages of the periovulatory period from women with normal menstrual cycles were used to assess the expression profile of *MMP14, MMP16,* and *MMP25*. The mRNA levels of *MMP14* in human granulosa cells showed a modest but significant increase by the late periovulatory stage compared to the preovulatory and early periovulatory stages, but no change was observed in the human theca cells across the periovulatory period (Fig. 2A). *MMP16* mRNA in the human granulosa cells showed a nearly 5-fold increase by the late ovulatory stage (Fig. 2B). In the theca cells, *MMP16* mRNA expression was not stimulated by hCG and decreased significantly by the postovulatory stage (Fig. 2B). No change in *MMP25* mRNA in granulosa cells was found; however, expression stayed steady through the late ovulatory stage and decreased by the postovulatory stage in theca cells (Fig. 2C).

In the macaque, granulosa cells collected from animals undergoing controlled ovarian stimulation were used to examine MT-MMP mRNA expression. The *MMP14* mRNA was detected in every granulosa cell sample examined; however, levels of *MMP14* mRNA did not change in response to hCG administration (Fig. 2D). In contrast to *MMP14*, hCG administration stimulated *MMP16* mRNA expression in macaque granulosa cells. *MMP16* mRNA levels were low at 0 h, increased to peak levels by 12 h after hCG administration, then declined to intermediate levels at 24–36 h after hCG (Fig. 2E). We utilized multiple primer sets to determine the expression profile of MMP25 in cynomolgus macaque granulosa cells but could not amplify a PCR product of appropriate size, whereas these primers yielded appropriate-size products in other tissues, such as spleen and lung (data not shown). It therefore appears that MMP25 is expressed at less than the detection limits of our real-time RT-PCR methodology.

Protein Expression Profile of MT-MMPs During the Periovulatory Period

Rat ovaries collected either before (0 h) or at different time points (8, 12, and 24 h) after hCG administration were used to analyze protein levels of MMP14 and MMP16. We focused on these two MT-MMPs because MMP25 did not change in the human. Two bands representing the active and proenzyme forms for both MMP14 and MMP16 proteins were detectable by immunoblotting (Fig. 3, A and C, respectively). Proprotein

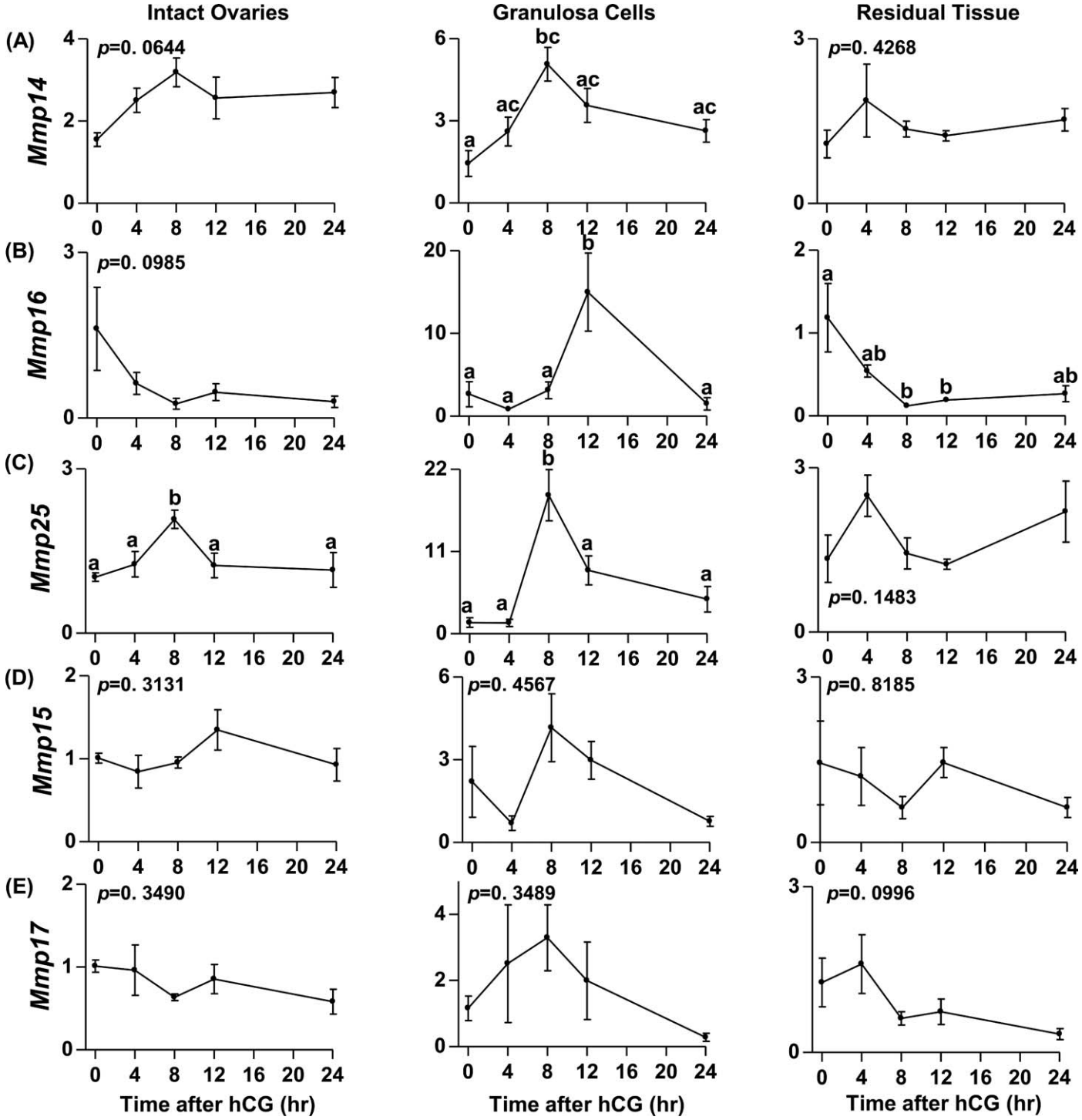

FIG. 1. Messenger RNA expression profiles of the MT-MMPs during the rat periovulatory period. The mRNA expression profiles of the MT-MMPs *Mmp14* (**A**), *Mmp16* (**B**), *Mmp25* (**C**), *Mmp15* (**D**), and *Mmp17* (**E**) in the intact ovary, granulosa cells, and residual ovarian tissue collected from eCG-primed immature rats at 0 h (48 h after eCG) or at 4, 8, 12, and 24 h after administration of hCG are shown. Relative levels of mRNA were normalized to L32 in each sample and expressed as the fold-change relative to 0 h. Data are presented as the mean ± SEM (n = 3–4 per time point) of the fold-change in mRNA levels, and different superscripts indicate significant changes ($P < 0.05$) in mRNA levels within an MT-MMP panel.

levels for both MMPs were low at 0 h and increased with hCG treatment, peaking at 12 h (Fig. 3, B and D). The active form of MMP14 showed a profile similar to that of its proform (Fig. 3B), whereas the active form of MMP16 peaked at 12 h post-hCG administration (Fig. 3D).

Macaque granulosa cells obtained 0, 12, 24, and 36 h after hCG administration were lysed and used to analyze proenzyme and active enzyme levels of MMP14 and MMP16 by immunoblotting. Bands representing the proform and active form of both MMP14 and MMP16 were detected (Fig. 4A). Levels of pro-MMP14 did not show any statistically significant changes either before or after hCG administration, although substantial variability was observed between monkeys (Fig. 4, A and B). Active MMP14 was low at 0 and 12 h after hCG,

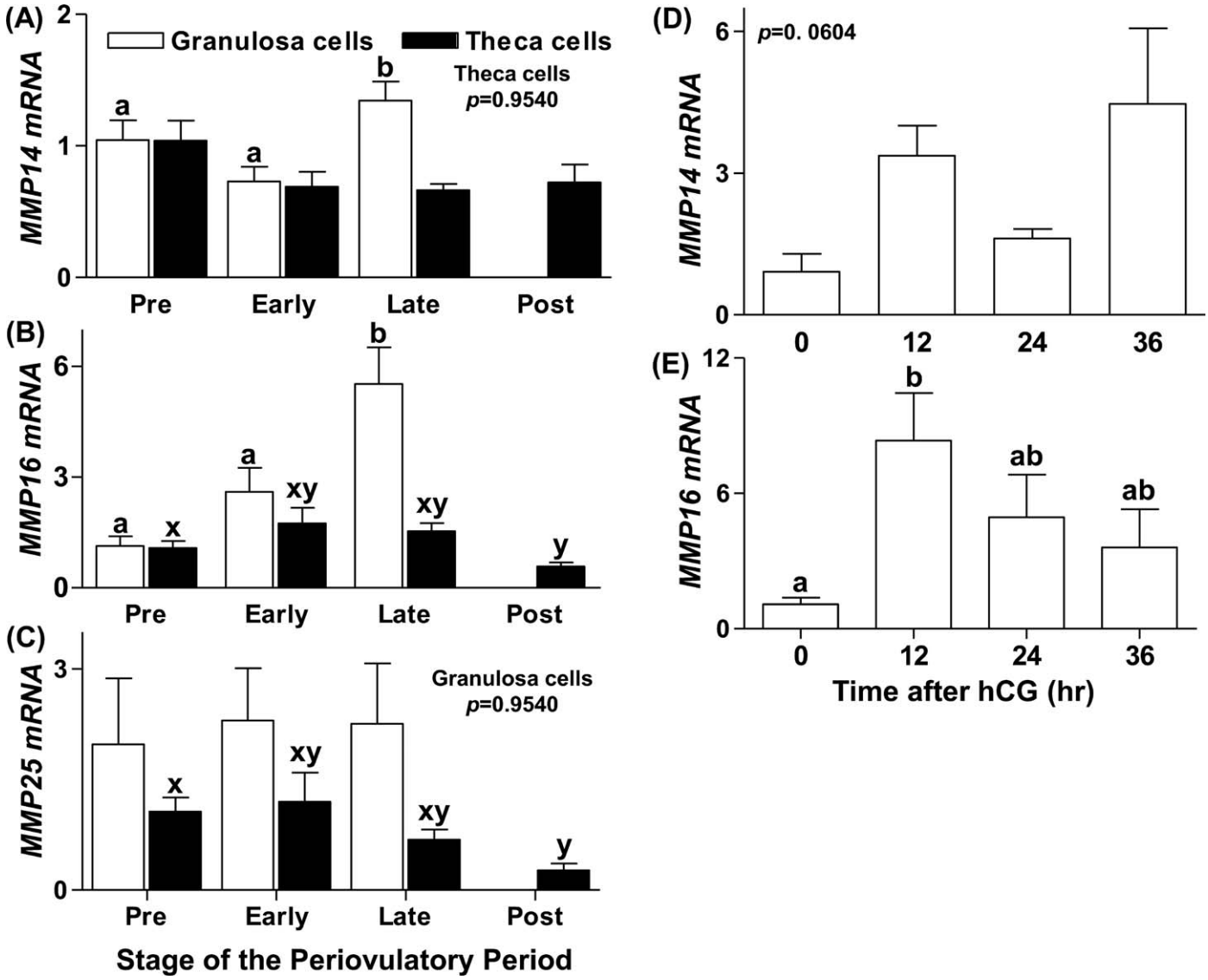

FIG. 2. Messenger RNA expression profiles of the MT-MMPs in human and macaque ovarian cells during the periovulatory period in vivo. Human granulosa and theca cells were collected from women undergoing elective surgery for tubal sterilization at different stages of the periovulatory period. The mRNA expression profiles of *MMP14* (**A**), *MMP16* (**B**), and *MMP25* (**C**) as determined by real-time RT-PCR in the granulosa (open bars) and theca (closed bars) cells are shown. Macaque granulosa cells were obtained 0, 12, 24, and 36 h after hCG administration from monkeys undergoing controlled ovarian stimulation and analyzed for *MMP14* (**D**) and *MMP16* (**E**). Relative levels of mRNA were normalized to GAPDH or L32 (for analysis of human or macaque samples, respectively) in each sample and expressed as the fold-change relative to the preovulatory stage or 0 h. Data are presented as the mean ± SEM (n = 3–4 per time point) of the fold-change in mRNA levels, and different superscripts indicate significant changes ($P < 0.05$) in mRNA levels.

increased by 24 h, and reached maximal expression at 36 h (Fig. 4B). Proenzyme levels of MMP16 followed a pattern similar to that of *MMP16* mRNA in the macaque granulosa cells, with low levels at 0 h, then increasing 7-fold to peak 12–24 h after hCG administration (Fig. 4C). Surprisingly, levels of active MMP16 were low (0.71 ± 0.26) and did not change with hCG administration (2.7 ± 1.0 arbitrary units) (Fig. 4C). Protein analysis could not be performed in humans due to unavailability of granulosa cells, theca cells, or intact ovary lysates.

Immunolocalization of MMP14, MMP16, and MMP25 in the Periovulatory Follicle

The MMP14 protein was detected during the periovulatory period of the rat ovary using an antibody raised against the hinge region of the protein that detects both the proform and active form of this enzyme. MMP14 immunostaining was weakly detected in the granulosa and theca cells of the preovulatory follicles at 0 h (Fig. 5, A and B). By 12 h after treatment with hCG, intense immunostaining was noted in the granulosa and theca cells of the ovulating follicles (Fig. 5, C and D). Omission of the primary antibody against MMP14 did not produce any staining (Fig. 5A, inset). MMP16 protein was also detected in the rat periovulatory-stage ovary using an antibody raised against the hinge region of the protein. MMP16 protein was detectable in the granulosa and theca cells at 0 h (Fig. 5, E and F). By 12 h after hCG, immunodetection of MMP16 was observed in all layers of the granulosa cells and theca cells, with intense staining in the granulosa cells (Fig. 5, G and H). In sections incubated without the primary antibody against MMP16, no staining was detected (Fig. 5E, inset). MMP25 protein was observed in the rat periovulatory ovary in the granulosa and theca cells at 0 h (Fig. 5, I and J). By 12 h

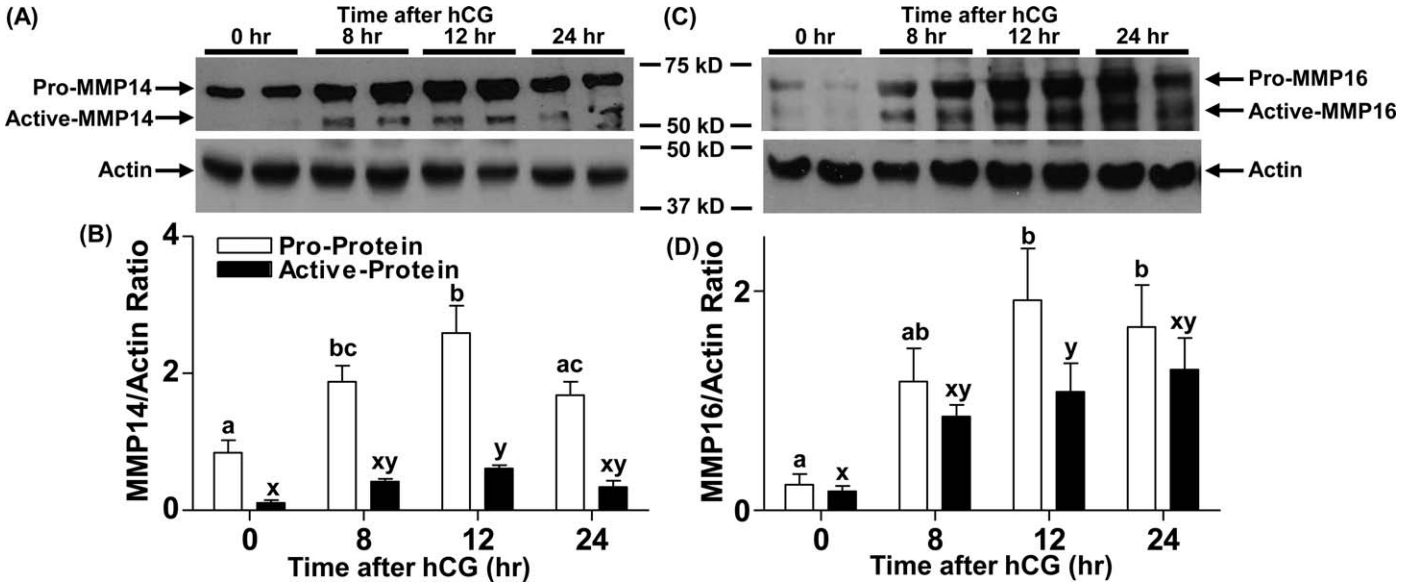

FIG. 3. Changes in MMP14 and MMP16 protein levels in rat ovaries during the periovulatory period. Rat ovaries were obtained 0, 8, 12, and 24 h after hCG administration from eCG-primed rats and processed for protein analysis. Representative immunoblots of MMP14 and MMP16 in the rat ovarian lysates at different times after hCG administration (top blots in **A** and **C**, respectively) are shown. The beta-actin immunoblots are from the respective blots obtained after stripping of the primary MMP antibodies (bottom blots in **A** and **C**) are also shown. Densitometric analysis was used to semiquantitate the changes in pro-MMP14 and active MMP14 (**B**) and in pro-MMP16 and active MMP16 (**D**). Arbitrary optical density units measured for proform and active form using ImageJ software were normalized to those measured for the internal control beta-actin. The graph depicts the mean ± SEM (n = 4 animals/group). Groups with no common letters are significantly different ($P < 0.05$).

after hCG, immunodetection of MMP25 was prominent in the mural granulosa cells (Fig. 5, K and L). In sections incubated without the primary antibody against MMP25, no staining was detected (Fig. 5I, inset).

The MMP14 protein was immunolocalized in human follicles collected from either the preovulatory or late ovulatory stage. Staining for MMP14 in the preovulatory follicle was mostly present in the stroma, whereas both granulosa and theca cells had minimal to no staining (Fig. 6A). Administration of hCG resulted in concentrated MMP14 staining in the granulosa and theca cells (Fig. 6B). MMP16 in the human follicles was also detected by immunohistochemistry using an antibody raised against the hinge region of the protein. Immunoreactive MMP16 was detectable in the granulosa and theca cells from the preovulatory stage (Fig. 6D), with intense staining in the granulosa cells after hCG administration by the late ovulatory stages (Fig. 6E). Omission of the primary antibody against both MMP14 and MMP16 did not show any staining (Fig. 6, C and F, respectively). Immunoreactive MMP25 was observed in the granulosa and theca cells in follicles collected after hCG administration in the preovulatory and late ovulatory stage but showed no change between these two stages (Fig. 6, G and H). Omission of the primary antibody resulted in a lack of staining (Fig. 6I).

Immunofluorescence using an antibody recognizing both pro-MMP14 and active MMP14 was performed to localize MMP14 proteins in the monkey periovulatory follicle (Fig. 7, A–D). MMP14 was weakly detected in granulosa cells of periovulatory follicles obtained 0 h after hCG (Fig. 7A). Stronger MMP14 immunodetection was visible in the granulosa cells of follicles obtained 12–36 h after hCG administration (Fig. 7, B–D). MMP16 was detected in the cells of monkey follicles by immunofluorescence, also using an antibody that recognizes both the proform and active form of this protein (Fig. 7, E–H). In granulosa cells of follicles obtained at 0 h, MMP16 immunoreactivity was similar to the background immunofluorescence. However, MMP16 was easily detected in granulosa cells of follicles obtained 12, 24, and 36 h after administration of hCG (Fig. 7, F–H, respectively). Omission of the primary antibody against both MMP14 and MMP16 did not show any staining (insets in Fig. 7, B and H, respectively). Immunolocalization of MMP25 in macaque ovary was not undertaken because we could not detect its mRNA in the granulosa cells.

DISCUSSION

One of the requirements for ovulation to occur is the localized expression of proteases, such as the plasmin, MMP, and ADAMTS family members in the ovary [1]. Many of these proteases increase after the ovulatory stimulus/LH surge [1, 4, 7, 15, 19]. However, the expression profiles of the members of the unique MMPs found on the cell surface, the MT-MMPs, have not been thoroughly examined in the ovary during the periovulatory period of any species. In the present study, we address this lacuna and, to our knowledge for the first time, demonstrate the expression profile of all the members of the MT-MMP subfamily across the rat periovulatory period and compare ovarian expression of key MT-MMPs in rats, monkeys, and humans. Previous reports have shown that MMP14 is induced during the periovulatory period of rodents and cows [20–23], and in this report, we show for the first time, that both MMP14 and MMP16 are increased in rat, macaque, and human granulosa cells.

The ovulatory process in rats and primates, which includes both humans and macaques, has an identical inducer, which is the LH surge in natural cycles and hCG administration in stimulated cycles [24]. Where these two taxa differ is the duration of the periovulatory period, which lasts approximately 14–16 h in rats and approximately 40 h in primates [18, 25, 26]. It has been recently suggested that similarities exist between these species in activities that lead to ovulation, although the molecular players utilized to achieve the end results could be different [24]. One striking example is the

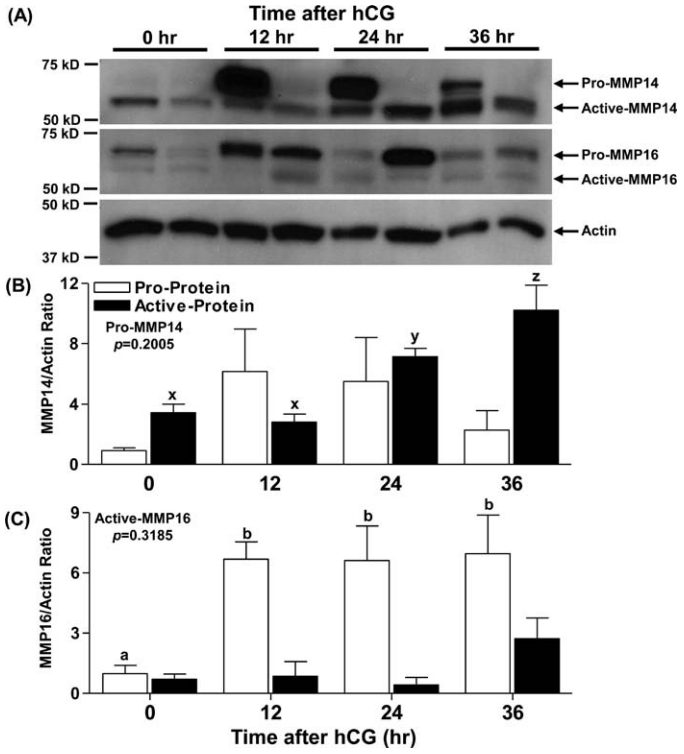

FIG. 4. Changes in MMP14 and MMP16 protein levels in macaque granulosa cells during the periovulatory period. Monkey granulosa cells were obtained 0, 12, 24, and 36 h after hCG administration from monkeys undergoing controlled ovarian stimulation and processed for protein analysis. A representative immunoblot of MMP14 and MMP16 along with pan-actin (**A**) in granulosa cell lysates at different times after hCG administration is shown. Densitometry was used to semiquantitate changes in pro-MMP14 and active MMP14 (**B**) as well as pro-MMP16 and active MMP16 (**C**) protein in granulosa cell lysates. Arbitrary optical density units measured for proform and active form were normalized to those measured for the internal control actin. The graph depicts the mean ± SEM (n = 4 animals/group). Groups with no common letters are significantly different ($P < 0.05$).

difference in the regulation and functional role of the protease ADAMTS1 between rodents and primates [24]**.** In rodents, *Adamts1* mRNA is induced between 6 and 12 h after hCG in a progesterone-dependent manner [27, 28]. However, in the macaque, the increase in *ADAMTS1* mRNA occurs only after ovulation and appears to have no progesterone dependency in the regulation of its gene expression [7, 29]. Importantly, the present study demonstrates that the mRNA expression of *MMP16* is conserved between rats, macaques, and humans. Additionally, the increase in the MMP14 active protein in both rats and macaques suggests that the functional role of this protein is maintained between species. In contrast, the periovulatory mRNA expression of *MMP25* does not appear to be conserved, which may be related to its function, as discussed below.

The MMP14 protein has been the most widely studied MT-MMP in the ovary to date. However, conflicting reports exist regarding the ovarian expression of this MT-MMP during the periovulatory period. In the present study, *MMP14* mRNA increased in isolated rat and human granulosa cells after hCG administration. In intact rat ovaries, an increase in MMP14 protein was found by 8 h post-hCG. These findings are similar to previous reports that *Mmp14* mRNA increases in the whole ovary following hCG treatment in rats [21, 23]. However, these previous studies showed that *MMP14* transcripts mostly localized to the theca cells of the preovulatory follicles, not to the granulosa cells [21, 23]. In contrast, our immunolocalization studies in rats, humans, and macaques showed intense immunostaining for MMP14 protein in both granulosa and theca cells after hCG treatment. Likewise, in other species, an increase in *MMP14* mRNA expression in bovine follicular tissue as well as MMP14 protein in the medaka fish follicle was noted before ovulation [20, 30]. Localization of *MMP14* mRNA in bovine periovulatory follicles revealed expression of *MMP14* mRNA in the theca layer before the LH surge, with an induction in the granulosa cell layer following GnRH administration [20]. In contrast to the present findings in humans and rats, expression of *MMP14* mRNA in macaque granulosa cells did not statistically change after hCG administration. This lack of statistical significance may be related to the variability observed between monkeys. However, the trend ($P = 0.060$) and relative change in expression (>3-fold) were similar to those observed in rats and humans. A lack of induction of *Mmp14* mRNA by hCG has been reported in mice; Hagglund et al. [22] observed no change in *Mmp14* mRNA expression in mouse intact ovaries collected throughout the periovulatory period by Northern blot analysis.

Although the mRNA levels of *MMP14* did not change in macaque granulosa cells, an increase in the active form of MMP14 protein corresponded to the time of ovulation in both the macaque and the intact rat ovary. MT-MMPs, similar to other MMPs, are synthesized as zymogens that need to be cleaved to generate the active enzyme [3, 11]. This posttranslational regulation is one mechanism whereby enzyme activity can be regulated without corresponding changes in mRNA expression. This cleavage of zymogen is brought about by other proteases, such as plasmin and MMPs [3, 11]. The current findings indicate that MMP14 may be regulated posttranslationally rather than at the mRNA level in macaques and that this posttranslational activation of MMP14 may also be important in rodents. These reports, together with our data, suggest that MMP14 is increased in the ovary during the periovulatory period and could play an important role during ovulation.

Unlike MMP14, reports on the expression profiles of other MT-MMPs in the ovary are sparse. Other investigators have examined the expression of *MMP16* mRNA in human cumulus and mural granulosa cells collected at the time of in vitro fertilization [31]. In those studies, expression of *MMP16* mRNA in the cumulus cells was higher compared to that in the mural granulosa cells [31]. However, the assessment of *MMP16* mRNA was at a single time point immediately before ovulation. The present study demonstrates, to our knowledge for the first time, an increase in *MMP16* mRNA in granulosa cells after hCG treatment in humans, macaques, and rats. These data suggest that the functional role of MMP16 during ovulation is conserved in these three species. Further support for this concept is forthcoming from the conservation of protein structure for MMP16 as well as MMP14 across species, in contrast to MMP25 (Supplemental Figs. S1–S3; Supplemental Data are available online at www.biolreprod.org). Of particular interest is that important functional sites, such as the catalytic and metal binding sites, for MMP14 and MMP16 are highly conserved in humans (Supplemental Fig. S4), even though substantial differences exist in the overall protein structure between these two MT-MMPs (a 53% sequence homology exists between human MMP14 and MMP16).

The expression of MMP25 seems to be uniquely induced following hCG treatment in rats, whereas it did not change in the human granulosa cells and was less than the detection limit in macaque granulosa cells. This variance in the MMP25

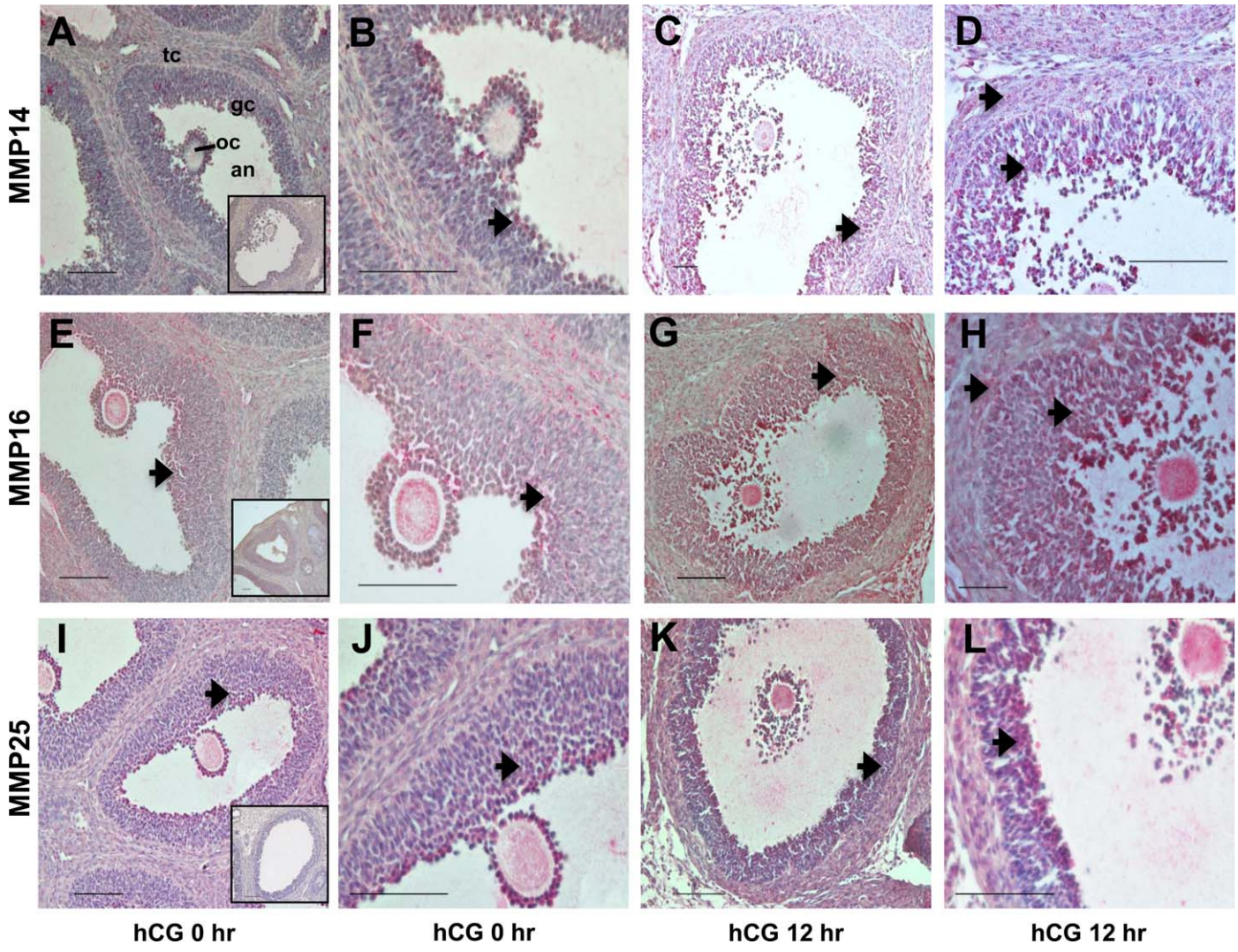

FIG. 5. Immunohistochemical detection of MMP14, MMP16, and MMP25 in the rat ovary during the periovulatory period. Ovaries collected from eCG-primed rats at different times after administration of an ovulatory dose of hCG were processed for immunolocalization of MMP14 (**A**–**D**), MMP16 (**E**–**H**), and MMP25 (**I**–**L**). In ovaries collected at 0 h (**A**, **B**, **E, F, I**, and **J**) and 12 h (**C**, **D**, **G**, **H**, **K**, and **L**) h after hCG administration, immunoreactive MMP14, MMP16, and MMP25 protein are identified as a red reaction product (arrows). **B**, **D**, **F**, **H**, **J**, and **L** are higher-magnification views (×40) of the images in **A**, **C**, **E**, **G**, **I**, and **K** (×20), respectively. Insets in **A**, **E**, and **I** are ovary sections in which the primary antibodies against MMP14, MMP16, and MMP25, respectively, were omitted. The full preovulatory (0 h) or periovulatory (12 h) ovarian follicle is shown (gc, granulosa cell layer; tc, theca cell layer; an, follicular antrum; oc, oocyte). Representative photomicrographs are shown for each time point. Bar = 50 μm (×20 panels) and 100 μm (×40 panels).

expression pattern could stem from differences in the inflammatory response during the ovulatory process that exist between species. MMP25 is predominantly expressed in the peripheral blood leukocytes and therefore is also called a leukolysin [32]. Being highly expressed in the leukocytes, the increase in *Mmp25* expression in the rat ovary could reflect, in part, the influx of leukocytes that occurs following hCG treatment [33, 34]. The magnitude of this inflammatory response and the massive increase in leukocytes observed in rats [34] may account for the increase in *Mmp25* mRNA expression in rats that is not observed in monkeys or humans. Because MMP25 is highly abundant in neutrophils, Starr et al. [35] proposed that this cell surface MMP is involved in the proteolytic regulation of specific inflammatory molecules involved in innate immune processes. In support of this postulate, they found 72 new substrates for MMP25, including chemokines that recruit neutrophils and monocytes, which is consistent with a role in the regulation of innate immune cellular responses [35]. These observations led to the proposal that MMP25 appears to be mainly involved in bioactive molecule cleavage rather than primarily regulating extracellular matrix homeostasis.

The observation that hCG treatment also increases *Mmp25* mRNA in isolated rat granulosa cells can be interpreted as indicating an induction in the granulosa cell compartment because *MMP25* has been reported in other tissues, such as the lung, spleen, and brain tumor cells [36]. Alternatively, expression of *Mmp25* in isolated granulosa cells may result from a carryover of leukocytes containing *Mmp25* during puncture of the follicles and extrusion and collection of the granulosa cells. Of interest, we were unable to induce *Mmp25* mRNA expression in granulosa cells isolated 48 h after eCG and stimulated with hCG (data not shown), which may reflect the leukocyte contribution of *Mmp25* in cells collected in vivo or the disruption of cell-cell contacts during granulosa cell isolation. That we were unable to induce mRNA expression of any of the MT-MMPs (*Mmp14*, *Mmp16*, or *Mmp25*) in vitro

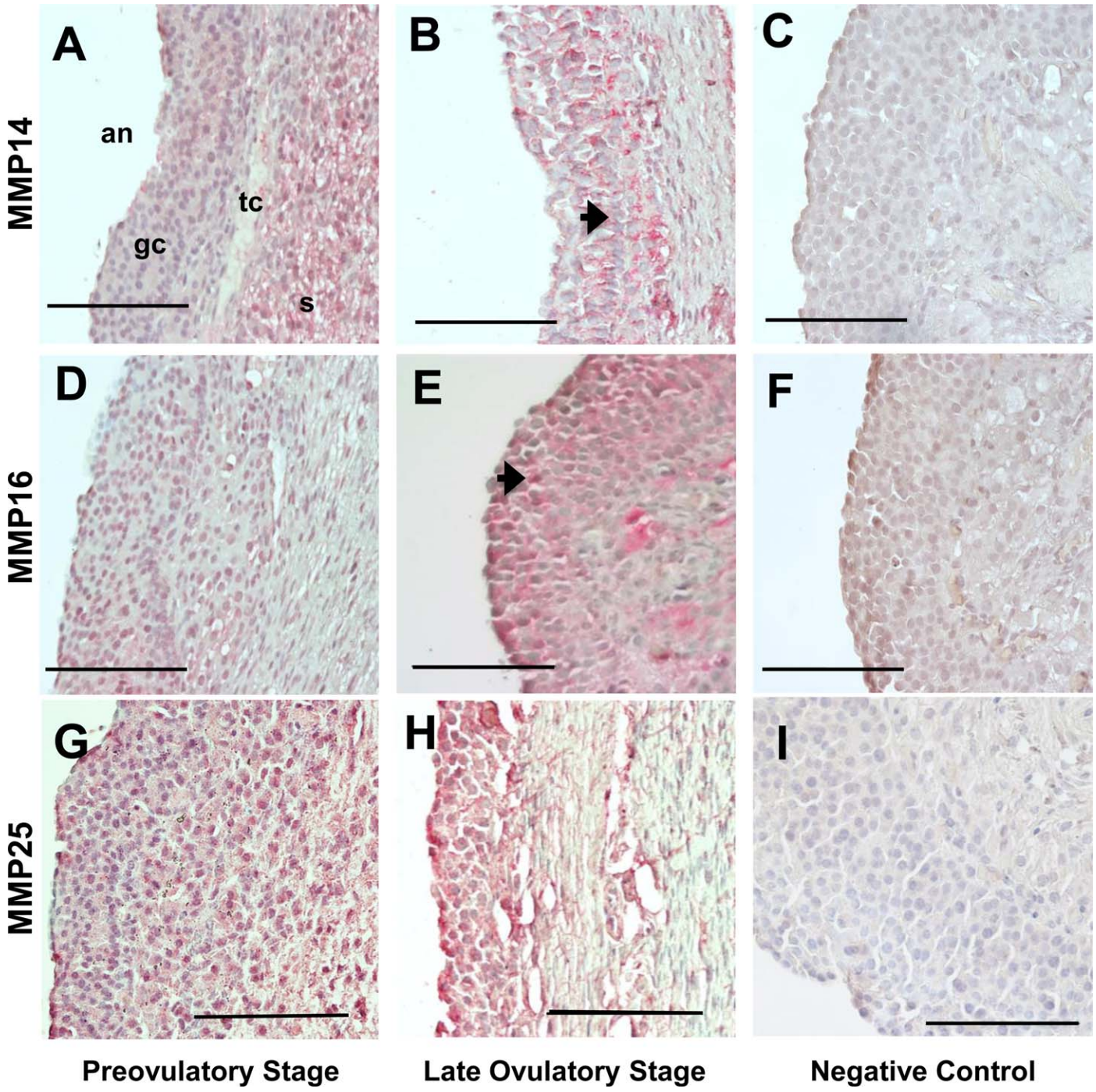

FIG. 6. Immunohistochemical detection of MMP14, MMP16, and MMP25 in human periovulatory follicles. Human follicles collected from women at different stages of the periovulatory period were processed for immunolocalization of MMP14, MMP16, and MMP25. Immunoreactive MMP14, MMP16, and MMP25 in follicles from preovulatory (**A**, **D**, and **G**) and late ovulatory (**B**, **E**, and **H**) stages, respectively, are identified as a red reaction product (arrow). **C**, **F**, and **I** represent follicle sections in which the primary antibodies against MMP14, MMP16, and MMP25, respectively, were omitted. All images are oriented as in **A**, with ovarian stroma (s), theca cells (tc), granulosa cells (gc), and follicle antrum (an) from right to left. Representative photomicrographs are shown for the different periovulatory stages. Bar =100 μm.

suggests that the in vitro culture system does not recapitulate the in vivo induction of these MT-MMPs.

We were able to detect the mRNAs for *Mmp15* and *Mmp17* in the rat ovary, but hCG administration did not elicit any changes in their expression levels. In humans, *MMP15* and *MMP17* mRNA expression has also been detected in the ovary [31, 37]. In the medaka fish ovary, however, MMP15 protein was detectable only in the granulosa cells of the ovulated follicles and not before ovulation [30]. No change in *Mmp17* mRNA following hCG administration has been reported in the mouse ovary [38], which is similar to the present findings in the rat ovary. Among the MT-MMPs, we were not able to detect the mRNA for *Mmp24* in the rat ovary either before or after hCG. This is in contrast to the report in medaka fish, where MMP24 transcripts and protein were present in small developing follicles [30, 39]. Based on our observation, it

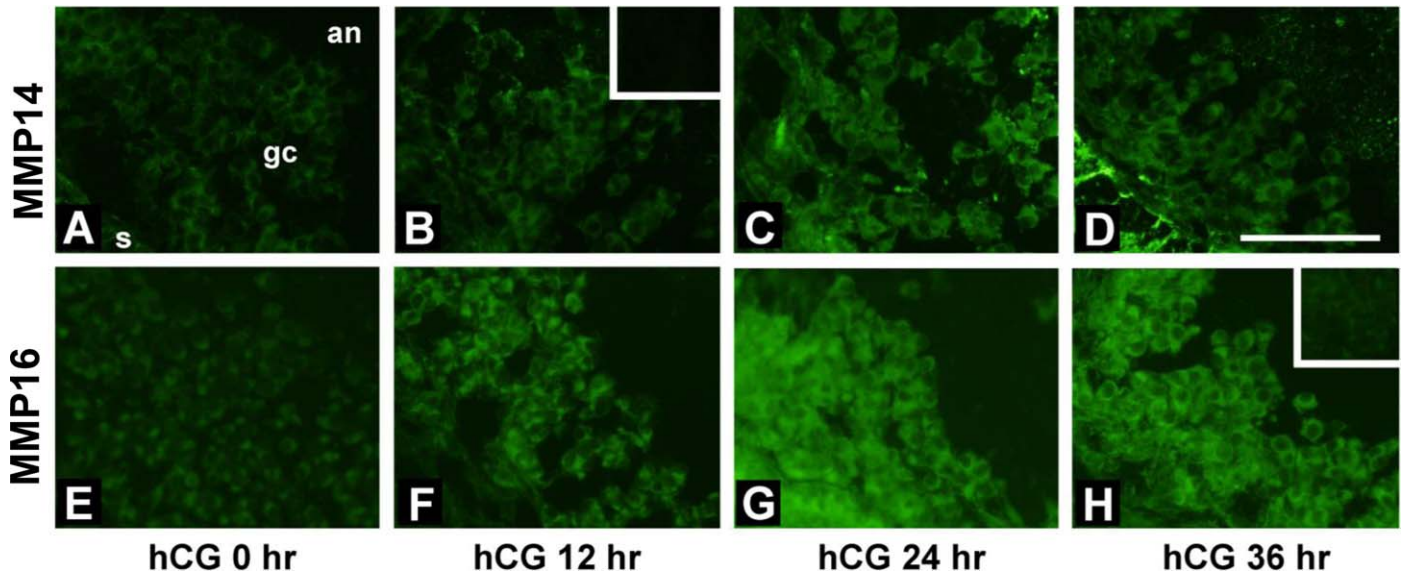

FIG. 7. Immunofluorescent detection of MMP14 and MMP16 in monkey periovulatory follicles. Monkeys received gonadotropins to stimulate the development of multiple follicles. Ovarian tissue from these animals was obtained before (0 h; **A** and **E**) or at 12 h (**B** and **F**), 24 h (**C** and **G**), or 36 h (**D** and **H**) after administration of hCG to initiate periovulatory events. Immunolocalization was performed for MMP14 (**A**–**D**) and MMP16 (**E**–**H**). All images are oriented as in **A**, with ovarian stroma (s) in the lower left, granulosa cells (gc) central, and follicle antrum (an) in the upper right. Insets in **B** and **H** show that faint immunofluorescence was present when the primary antibody was omitted. Bar = 50 μm.

appears that although only a select few MT-MMP mRNAs are increased by hCG during the periovulatory period, other MT-MMPs are still expressed and could function to aid during ovulation and corpus luteum formation.

The functional role of MT-MMPs has been extensively characterized in various systems, and they have been shown to break down matrix proteins, activate other proteases, as well as cause pericellular activation of growth factors and cytokines to influence various cellular processes [10–12]. Within the rat ovary, MMP14 has been shown to activate the gelatinase, MMP2 [21]. Additionally, all the MT-MMPs, with the exception of MMP17, have been shown to activate MMP2 in other systems [40]. That MMP25, which is a GPI-anchored MT-MMP, is able to activate MMP2 like the type I transmembrane-anchored MT-MMPs (MMPs 14–16 and 24) has led to the suggestion that MMP25 was more closely related to MMP14 than the other GPI-anchored MT-MMP, MMP17, and may share some of the functions of the type I MT-MMPs [41]. However, subsequent studies have demonstrated that MMP25 is a relatively weak activator of progelatinase, and in fact, MMP25 is closer in function to MMP3 (stromelysin-1) than MMP14 in terms of substrate and inhibitor specificity [41, 42].

In a manner similar to their role in activating other proteases, MT-MMPs can cause pericellular activation of growth factors and cytokines and breakdown of matrix proteins, influencing various cellular processes [10–12]. In the ovary, activation of growth factors such as epidermal growth factor-like ligands and cleavage of membrane proteins such syndecan-1 have been well documented to have a role in ovulation and formation of corpus luteum [43–46], suggesting that this may be another key role of MT-MMPs in the ovulatory process.

Recent studies have shown that MT-MMPs have a role that is independent of their protease activity. The MT-MMPs (MMPs 14–16 and 24) have intracytoplasmic domains that can act as adapter proteins, whereby interaction with the extracellular domain can influence the intracellular signal transduction. The MMP14 cytoplasmic domain has been shown to activate the ERK pathway [47], Rac1 [48] and HIF1α [49]. Thus, MT-MMPs can influence diverse cellular processes either dependent or independent of their proteolytic actions, thereby potentially influencing the various events occurring within the ovulating follicle.

Genetic approaches such as gene deletion/knockout studies have been used to determine the functional role of MMP14 and MMP16. Nullizygous mutations in MMP14 gene have led to postnatal or premature death, with severe skeletal abnormalities [50]. Because of these pleiotropic defects, a direct reproductive phenotype has not been apparent, so additional studies are required utilizing an ovarian or granulosa-specific conditional knockout for this gene. In contrast, MMP16 knockouts had similar retardation in skeletal growth but were fertile [51]. This might stem from the fact that MMP16 function could be compensated by other MMPs, including MMP14 [51]. Although MMPs are a diverse group, they share structural and functional similarities [3]. Because of this redundancy among MMPs, mice lacking specific MMPs have not yielded any significant insights into the ovulatory process [52]. In fact, a diverse number of MMPs are induced during the periovulatory period of rats, macaques, and humans. In rats, other MMPs, such as MMPs 1, 2, 10, 13, and 19, are increased by an ovulatory stimulus [1, 3, 19]. In macaques, MMP family members that are induced by hCG include MMPs 1, 2, 7, 9, 10, and 19 [2, 7]. In the human ovary, MMPs 2, 9, and 10 are among the proteases that increase during the periovulatory period [15]. All these different MMPs are induced during the periovulatory period either before or at the time of ovulation. Similarly, MMP14 is induced early (8 h), whereas MMP16 is induced late (12 h), during the periovulatory period of the rat.

During ovulation, the ovary undergoes dynamic changes that require basement membrane breakdown to permit oocyte release and cellular migration, differentiation, and vascularization to form the corpus luteum [18, 53, 54]. Our report shows, to our knowledge for the first time, that members of the MT-MMP subfamily other than MMP14 are also expressed in the ovulating ovary and that the expression of select subfamily members is increased by hCG administration. By virtue of their

expression and localization pattern during the periovulatory period, we postulate that these MMPs are important for ovulation and corpus luteum formation. These MMPs could potentially function by participating in follicular wall breakdown either directly or indirectly through activating other enzymes, modulating growth factor availability or stimulating intracellular signaling pathways and thereby influencing a myriad of cellular processes in an ovulating follicle.

ACKNOWLEDGMENT

The r-hFSH and Ganirelix were generously provided by Organon and Schering-Plough, respectively, both of which are divisions of Merck & Co. Serono Reproductive Biology Institute kindly provided r-hLH, r-hCG, and Antide. The authors thank Drs. Misung Jo and Birendra Mishra for critically reading the manuscript and Dr. Jiyeon Park for help with the immunoblotting.

REFERENCES

1. Curry TE Jr, Smith MF. Impact of extracellular matrix remodeling on ovulation and the folliculo-luteal transition. Semin Reprod Med 2006; 24: 228–241.
2. Chaffin CL, Stouffer RL. Expression of matrix metalloproteinases and their tissue inhibitor messenger ribonucleic acids in macaque periovulatory granulosa cells: time course and steroid regulation. Biol Reprod 1999; 61: 14–21.
3. Curry TE Jr, Osteen KG. The matrix metalloproteinase system: changes, regulation, and impact throughout the ovarian and uterine reproductive cycle. Endocr Rev 2003; 24:428–465.
4. Liu YX. Plasminogen activator/plasminogen activator inhibitors in ovarian physiology. Front Biosci 2004; 9:3356–3373.
5. Mittaz L, Russell DL, Wilson T, Brasted M, Tkalcevic J, Salamonsen LA, Hertzog PJ, Pritchard MA. *Adamts-1* is essential for the development and function of the urogenital system. Biol Reprod 2004; 70:1096–1105.
6. Guerre EF Jr, Clark MR, Muse KN, Curry TE Jr. Intrabursal administration of protein kinase or proteinase inhibitors: effects on ovulation in the rat. Fertil Steril 1991; 56:126–133.
7. Peluffo MC, Murphy MJ, Baughman ST, Stouffer RL, Hennebold JD. Systematic analysis of protease gene expression in the rhesus macaque ovulatory follicle: metalloproteinase involvement in follicle rupture. Endocrinology 2011; 152:3963–3974.
8. Nagase H, Woessner JF Jr. Matrix metalloproteinases. J Biol Chem 1999; 274:21491–21494.
9. Visse R, Nagase H. Matrix metalloproteinases and tissue inhibitors of metalloproteinases: structure, function, and biochemistry. Circ Res 2003; 92:827–839.
10. Sternlicht MD, Werb Z. How matrix metalloproteinases regulate cell behavior. Annu Rev Cell Dev Biol 2001; 17:463–516.
11. Zucker S, Pei D, Cao J, Lopez-Otin C. Membrane type-matrix metalloproteinases (MT-MMP). Curr Top Dev Biol 2003; 54:1–74.
12. Sounni NE, Noel A. Membrane type-matrix metalloproteinases and tumor progression. Biochimie 2005; 87:329–342.
13. Vandevoort CA, Baughman WL, Stouffer RL. Comparison of different regimens of human gonadotropins for superovulation of rhesus monkeys: ovulatory response and subsequent luteal function. J In Vitro Fertilization Embryo Transfer 1989; 6:85–91.
14. Chaffin CL, Hess DL, Stouffer RL. Dynamics of periovulatory steroidogenesis in the rhesus monkey follicle after ovarian stimulation. Hum Reprod 1999; 14:642–649.
15. Lind AK, Dahm-Kahler P, Weijdegard B, Sundfeldt, Brannstrom M. Gelatinases and their tissue inhibitors during human ovulation: increased expression of tissue inhibitor of matrix metalloproteinase-1. Mol Hum Reprod 2006; 12:725–736.
16. Livak KJ, Schmittgen TD. Analysis of relative gene expression data using real-time quantitative PCR and the 2(−Delta Delta C(T)) Method. Methods 2001; 25:402–408.
17. Rosewell KL, Li F, Puttabyatappa M, Akin JW, Brannstrom M, Curry TE Jr. Ovarian expression, localization, and function of tissue inhibitor of metalloproteinase 3 (TIMP3) during the periovulatory period of the human menstrual cycle. Biol Reprod 2013; 89:121.
18. Richards JS. Ovulation: new factors that prepare the oocyte for fertilization. Mol Cell Endocrinol 2005; 234:75–79.
19. McCord LA, Li F, Rosewell KL, Brannstrom M, Curry TE Jr. Ovarian expression and regulation of the stromelysins during the periovulatory period in the human and the rat. Biol Reprod 2012; 86:78.
20. Bakke LJ, Dow MP, Cassar CA, Peters MW, Pursley JR, Smith GW. Effect of the preovulatory gonadotropin surge on matrix metalloproteinase (MMP)-14, MMP-2, and tissue inhibitor of metalloproteinases-2 expression within bovine periovulatory follicular and luteal tissue. Biol Reprod 2002; 66:1627–1634.
21. Jo M, Thomas LE, Wheeler SE, Curry TE Jr. Membrane type 1-matrix metalloproteinase (MMP)-associated MMP-2 activation increases in the rat ovary in response to an ovulatory dose of human chorionic gonadotropin. Biol Reprod 2004; 70:1024–1032.
22. Hagglund AC, Ny A, Leonardsson G, Ny T. Regulation and localization of matrix metalloproteinases and tissue inhibitors of metalloproteinases in the mouse ovary during gonadotropin-induced ovulation. Endocrinology 1999; 140:4351–4358.
23. Liu K, Wahlberg P, Ny T. Coordinated and cell-specific regulation of membrane type matrix metalloproteinase 1 (MT1-MMP) and its substrate matrix metalloproteinase 2 (MMP-2) by physiological signals during follicular development and ovulation. Endocrinology 1998; 139: 4735–4738.
24. Chaffin CL, Vandevoort CA. Follicle growth, ovulation, and luteal formation in primates and rodents: a comparative perspective. Exp Biol Med 2013; 238:539–548.
25. Weick RF, Dierschke DJ, Karsch FJ, Butler WR, Hotchkiss J, Knobil E. Periovulatory time courses of circulating gonadotropic and ovarian hormones in the rhesus monkey. Endocrinology 1973; 93:1140–1147.
26. Chaffin CL, Stouffer RL. Local role of progesterone in the ovary during the periovulatory interval. Rev Endocr Metab Disord 2002; 3:65–72.
27. Espey LL, Yoshioka S, Russell DL, Robker RL, Fujii S, Richards JS. Ovarian expression of a disintegrin and metalloproteinase with thrombospondin motifs during ovulation in the gonadotropin-primed immature rat. Biol Reprod 2000; 62:1090–1095.
28. Doyle KM, Russell DL, Sriraman V, Richards JS. Coordinate transcription of the ADAMTS-1 gene by luteinizing hormone and progesterone receptor. Mol Endocrinol 2004; 18:2463–2478.
29. Young KA, Tumlinson B, Stouffer RL. ADAMTS-1/METH-1 and TIMP-3 expression in the primate corpus luteum: divergent patterns and stage-dependent regulation during the natural menstrual cycle. Mol Hum Reprod 2004; 10:559–565.
30. Ogiwara K, Takano N, Shinohara M, Murakami M, Takahashi T. Gelatinase A and membrane-type matrix metalloproteinases 1 and 2 are responsible for follicle rupture during ovulation in the medaka. Proc Natl Acad Sci U S A 2005; 102:8442–8447.
31. Koks S, Velthut A, Sarapik A, Altmae S, Reinmaa E, Schalkwyk LC, Fernandes C, Lad HV, Soomets U, Jaakma U, Salumets A. The differential transcriptome and ontology profiles of floating and cumulus granulosa cells in stimulated human antral follicles. Mol Hum Reprod 2010; 16: 229–240.
32. Pei D. Leukolysin/MMP25/MT6-MMP: a novel matrix metalloproteinase specifically expressed in the leukocyte lineage. Cell Res 1999; 9:291–303.
33. Brannstrom M, Norman RJ. Involvement of leukocytes and cytokines in the ovulatory process and corpus luteum function. Hum Reprod 1993; 8: 1762–1775.
34. Oakley OR, Kim H, El-Amouri I, Lin PC, Cho J, Bani-Ahmad M, Ko C. Periovulatory leukocyte infiltration in the rat ovary. Endocrinology 2010; 151:4551–4559.
35. Starr AE, Bellac CL, Dufour A, Goebeler V, Overall CM. Biochemical characterization and N-terminomics analysis of leukolysin, the membrane-type 6 matrix metalloprotease (MMP25): chemokine and vimentin cleavages enhance cell migration and macrophage phagocytic activities. J Biol Chem 2012; 287:13382–13395.
36. Velasco G, Cal S, Merlos-Suarez A, Ferrando AA, Alvarez S, Nakano A, Arribas J, Lopez-Otin C. Human MT6-matrix metalloproteinase: identification, progelatinase A activation, and expression in brain tumors. Cancer Res 2000; 60:877–882.
37. Puente XS, Pendas AM, Llano E, Velasco G, Lopez-Otin C. Molecular cloning of a novel membrane-type matrix metalloproteinase from a human breast carcinoma. Cancer Res 1996; 56:944–949.
38. Richards JS, Hernandez-Gonzalez I, Gonzalez-Robayna I, Teuling E, Lo Y, Boerboom D, Falender AE, Doyle KH, LeBaron RG, Thompson V, Sandy JD. Regulated expression of ADAMTS family members in follicles and cumulus oocyte complexes: evidence for specific and redundant patterns during ovulation. Biol Reprod 2005; 72:1241–1255.
39. Kimura A, Shinohara M, Ohkura R, Takahashi T. Expression and localization of transcripts of MT5-MMP and its related MMP in the ovary of the medaka fish *Oryzias latipes*. Biochim Biophys Acta 2001; 1518: 115–123.

40. Morrison CJ, Overall CM. TIMP independence of matrix metalloproteinase (MMP)-2 activation by membrane type 2 (MT2)-MMP is determined by contributions of both the MT2-MMP catalytic and hemopexin C domains. J Biol Chem 2006; 281:26528–26539.
41. Nie J, Pei D. Direct activation of pro-matrix metalloproteinase-2 by leukolysin/membrane-type 6 matrix metalloproteinase/matrix metalloproteinase 25 at the asn(109)-Tyr bond. Cancer Res 2003; 63:6758–6762.
42. English WR, Velasco G, Stracke JO, Knauper V, Murphy G. Catalytic activities of membrane-type 6 matrix metalloproteinase (MMP25). FEBS Lett 2001; 491:137–142.
43. Conti M, Hsieh M, Park JY, Su YQ. Role of the epidermal growth factor network in ovarian follicles. Mol Endocrinol 2006; 20:715–723.
44. Puttabyatappa M, Brogan RS, Vandevoort CA, Chaffin CL. EGF-like ligands mediate progesterone's anti-apoptotic action on macaque granulosa cells. Biol Reprod 2013; 88:18.
45. Watson LN, Mottershead DG, Dunning KR, Robker RL, Gilchrist RB, Russell DL. Heparan sulfate proteoglycans regulate responses to oocyte paracrine signals in ovarian follicle morphogenesis. Endocrinology 2012; 153:4544–4555.
46. Akison LK, Alvino ER, Dunning KR, Robker RL, Russell DL. Transient invasive migration in mouse cumulus oocyte complexes induced at ovulation by luteinizing hormone. Biol Reprod 2012; 86:125.
47. D'Alessio S, Ferrari G, Cinnante K, Scheerer W, Galloway AC, Roses DF, Rozanov DV, Remacle AG, Oh ES, Shiryaev SA, Strongin AY, Pintucci G, et al. Tissue inhibitor of metalloproteinases-2 binding to membrane-type 1 matrix metalloproteinase induces MAPK activation and cell growth by a non-proteolytic mechanism. J Biol Chem 2008; 283:87–99.
48. Gonzalo P, Guadamillas MC, Hernandez-Riquer MV, Pollan A, Grande-Garcia A, Bartolome RA, Vasanji A, Ambrogio C, Chiarle R, Teixido J, Risteli J, Apte SS, et al. MT1-MMP is required for myeloid cell fusion via regulation of Rac1 signaling. Dev Cell 2010; 18:77–89.
49. Sakamoto T, Seiki M. A membrane protease regulates energy production in macrophages by activating hypoxia-inducible factor-1 via a non-proteolytic mechanism. J Biol Chem 2010; 285:29951–29964.
50. Holmbeck K, Bianco P, Caterina J, Yamada S, Kromer M, Kuznetsov SA, Mankani M, Robey PG, Poole AR, Pidoux I, Ward JM, Birkedal-Hansen H. MT1-MMP-deficient mice develop dwarfism, osteopenia, arthritis, and connective tissue disease due to inadequate collagen turnover. Cell 1999; 99:81–92.
51. Shi J, Son MY, Yamada S, Szabova L, Kahan S, Chrysovergis K, Wolf L, Surmak A, Holmbeck K. Membrane-type MMPs enable extracellular matrix permissiveness and mesenchymal cell proliferation during embryogenesis. Dev Biol 2008; 313:196–209.
52. Curry TE Jr. ADAMTS1 and versican: partners in ovulation and fertilization. Biol Reprod 2010; 83:505–506.
53. Stocco C, Telleria C, Gibori G. The molecular control of corpus luteum formation, function, and regression. Endocr Rev 2007; 28:117–149.
54. Stouffer RL, Chandrasekher YA, Slayden OD, Zelinski-Wooten MB. Gonadotrophic and local control of the developing corpus luteum in rhesus monkeys. Hum Reprod 1993; 8(suppl 2):107–111.